Rheology of Aqueous Silicon Nitride Suspensions

Alwin Nagel,* Günter Petzow‡

Max-Planck-Institut für Metallforschung, Institut für Werkstoffwissenschaft, Pulvermetallurgisches Laboratorium, Heisenbergstr. 5, D-7000 Stuttgart 80, FRG

&

Peter Greil

Technische Universität Hamburg-Harburg Arbeitsbereich Technische Keramik Harburger Schloßstr. 20, D-2100 Hamburg 90, FRG

Abstract

Highly concentrated silicon nitride slips with solid-volume concentrations ϕ of up to 0·475 were prepared from preoxidized, submicron powders in aqueous solutions at pH > 8. Viscosity measurements reveal a pseudo-plastic flow behaviour at ϕ > 0·35, which could not be described by existing flow equations. On the basis of the elastic-floc model for highly concentrated suspensions, a modified flow equation was derived, which is only determined by the initial floc-volume ratio and the particle-packing density. The calculated viscosity fits very well with the experimental values from low to high particle-volume concentrations ϕ from 0·2 to 0·475.

Hochkonzentrierte Siliziumnitridschlicker mit Feststoffgehalten bis zu einem Durchmesser von 0·475 wurden aus voroxidierten Submicronpulvern in wässerigen Suspensionen mit pH > 8 hergestellt. Die Viskositätsmessungen zeigen ein pseudoplastisches Fließverhalten für ϕ > 0·35, das durch bekannte Fließgrenze nicht beschrieben werden konnte. Basierend auf dem elastischen Flockenmodell für hochkonzentrierte Suspensionen wurde ein modifiziertes Fließgesetz aufgestellt, das nur durch das anfängliche Flockenvolumenverhältnis und der Teilchenpackungsdichte abhängt. Die berechneten Viskositäten stimmen gut mit den experimentellen Ergebnissen von niedrigen bis zu hohen Volumenkonzentrationen der Teilchen ($\phi = 0·2$–$0·475$) überein.

* Present address: Feldmuehle AG, Plochingen, FRG.
‡ To whom all correspondence should be addressed.

1 Introduction

Silicon-nitride-based ceramics are considered as one of the most promising high-temperature-resistant, high-stress-resistant materials for applications in heat engines. Though the material has generally proved its capability as a high-temperature structural material, further improvement of high-temperature mechanical properties and in particular the reduction of their variations in large-scale production are required. Decreasing grain size and increasing purity of the multiphase silicon nitride powder mixtures make uncontrolled powder agglomeration, chemical heterogeneities, and contamination a severe problem, which ultimately determines the reproducibility of the fabrication

371

technology and the reliability of the material properties.

Colloidal-consolidation techniques of submicron-ceramic-powder suspensions generally gain in significance for the production of defect-free compacts with high green density and improved sintering properties.[1,2] The submicron-powder particles may be stabilized against rapid flocculation by generating repulsive forces between the solvated and isolated particles either due to electric double-layer formation in aqueous solutions[3] or steric or combined electrosteric hindrance of critical particle–particle approach in non-aqueous solutions.[4–6] Thus, aqueous slips of silicon nitride could be prepared at a pH of 8–10 by electrostatic stabilization, whereby the surface of the silicon nitride particles is negatively charged.[7] Highly concentrated slips are required to reduce the casting time and shrinkage of the drying sediment during slip-casting. With increasing powder concentration, however, the particle–particle interactions exert an increasing influence on the suspension stability in relation to rapid flocculation and on the rheological behaviour during casting.[8–13] In a coagulated colloidal system, the particles combine to form flocs and floc networks, which are termed aggregates. Slip-casting experiments of highly concentrated silicon nitride slips showed a pseudo-plastic flow behaviour, with pronounced Bingham stresses,[14] which may be related to the formation of a network structure of weakly bonded particle aggregates[15–17] with increasing particle–particle interaction.[15,16,18,19] If the sheared aggregates (flocs) are slowly reconstructing, the system may exhibit thixotropic behaviour.

Based on the analysis of the energy-dissipating process involved in overcoming the interactions between the particles and aggregates, flow models are derived to describe the flow behaviour of non-Newtonian suspensions such as the elastic-floc model.[15–17] Various empirical relations such as the Mooney, the Eilers, or the Dougherty–Krieger equations, were derived to describe the viscous-energy dissipation that is associated with the shear-dependent floc-structure dynamics in a suspension.[9,17,20,21] At high shear rates, additional energy-dissipative processes, such as floc orientation, stretching, and compression, may consume energy. The floc structure was found to be strongly dependent on the colloidal interaction forces between suspended particles,[15,16] which is confirmed by the strong influence of the electrokinetic potential on the flow behaviour of aqueous silicon nitride suspensions.[7]

Rheological measurements of slip viscosity and flow behaviour of concentrated silicon nitride slips may therefore be used to obtain information on the structure of the solid phase under shear motion. In particular, the deflocculation ratio, i.e. the ratio of isolated to coagulated primary and secondary particles and aggregates, exerts a dominant influence on the time- and shear-dependent casting properties of highly concentrated silicon nitride slips. It is the aim of the present work to investigate the rheology of very highly concentrated aqueous silicon nitride slips in order to understand the decisive influence of the solid concentration on the casting properties. On the basis of rheological measurements of the shear-stress–shear-rate relationship, a simple model will be developed, which relates the solid-phase structure to the viscosity of the slips. Thus, the slip-casting technology of submicron silicon nitride powders may be optimized with respect to improved green-compact homogeneity and defect-free micro-structures.

2 Experimental Procedure

2.1 Slip preparation

A submicron α-phase silicon nitride powder (LC 12, H.C. Starck, Berlin, FRG), containing 15 mass% of $Y_3Al_5O_{12}$ as sintering additive, was used for the slip preparation. Powder batches of 0·5–4 kg were milled in a polyamide attritor for 4 h in isopropanol, dried, and finally sieved at 250 μm. From this powder stock, the various slips with different solid concentrations were prepared. Figure 1 represents the results of the grain-size-distribution analyses as obtained from a laser-scattering granulometer (HR 850, Cilas-Alcatel, France). Prior to the measurement, the silicon nitride powder was ultra-sonicated for 15 min in an aqueous suspension with
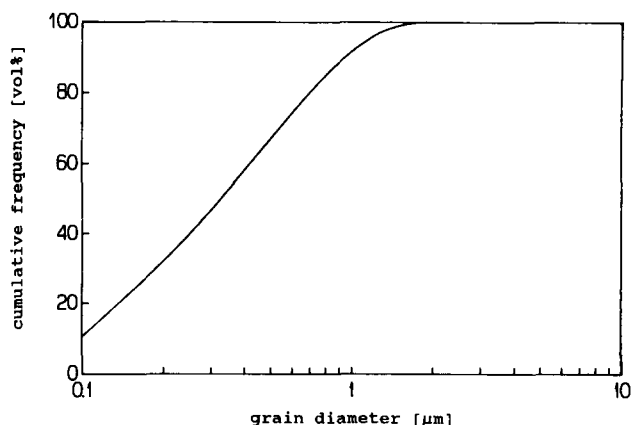

Fig. 1. Grain-size distribution of the silicon nitride powder mixture after milling.

a concentration of 200 mg powder in 1 litre. The milled powder is characterized by a mean grain diameter $d_{50} \approx 0.28\,\mu m$ and a specific surface area, measured according to the three-point BET method (Quantachrome, US), of $23.5\,m^2/g$ (Table 1).

Table 1. Powder characteristics

Powder	Producer	Specific surface area (BET) (m^2/g)
α-Si_3N_4 LC 12	H. C. Starck, FRG[a]	19.7
Y_2O_3 99.9	H. C. Starck, FRG	14.3
Al_2O_3 A 6	Ugine Kuhlmann, F	8
$Y_2Al_5O_{12}$[b]		10

[a] N, 38.4; O, 2.0; C, 0.17; Fe, 0.02; Al, 0.05; Ca, 0.01 wt%.
[b] Y_2O_3 (56.7%) + Al_2O_3 (43.3%), 4h/1400°C, 4h/800 min⁻¹ attritor milled.

The milled, dried, and sieved silicon nitride powder was added to the appropriate amount of microfiltrated, double-distilled water, small amounts of an ammonia solution, and an organic deflocculant. A polyelectrolytic surfactant (Dolapix PC 33, Zschimmer & Schwarz, Lahnstein, FRG) was used in a concentration of $5 \times 10^{-3}\,ml/g$. The functional groups in the polyacrylate were carboxylic groups, —COOH, which are completely dissociated[22] to negatively charged —COO⁻ groups at pH ≥ 8.5. A mass of 100–500 g of the slip was milled with wear-resistant zirconia balls (Y-TZP, $d = 8\,mm$) for 0.5–1 h in a planetary ball mill (Fritsch, Selb, FRG). The milling procedure resulted only in a destruction of large agglomerates, no further increase in the powder surface area being found.

2.2 Zetapotential and rheological measurements

The zetapotential, ζ, was calculated from the electrophoretic mobility according to the Smoluchowski equation.[23] The electrophoretic mobility was measured in diluted suspensions ($\phi < 10^{-5}$) at constant ionic strength. Prior to the measurement in a zetasizer II (Malvern, Cambridge, UK), the suspension was set to constant pH and ultrasonicated for 10 min.

Viscosity measurements were conducted with a rotary viscosimeter (Rotovisco RV 12, Haake, FRG) with a sample chamber MV DIN 53019. Shear rates of $D = 1.3$–$660\,s^{-1}$ were applied. For low-viscous slips with $\eta < 500\,mPa\,s$, the chamber unit NV ($D_{max} = 2770\,s^{-1}$) was used. The temperature was kept constant at $25 \pm 0.1°C$. The accuracy of the measurement equipment was examined by using calibration liquids of known viscosity (Haake, FRG). The measurement error is less than $\pm 10\%$ of

the absolute value, with a reproducibility better than 2%.

Flow curves were determined, starting for each measurement point with a steady-state floc structure of the suspension at the maximum shear rate D_{max} ($2770\,s^{-1}$). Each shear-stress value was taken after 10 s at constant shear rate. The Bingham-yield value τ_B and plastic viscosity η_{pl} were determined from the flow curves by linear regression in the interval $40 < D < 180\,s^{-1}$. For some suspensions, the shear rates were kept constant at $5.4\,s^{-1}$, and the shear stress was measured after 10 s and after 30 min. Large differences between the initial and the later shear stress were assumed to be due to thixotropic effects.

3 Results

It has been shown[7] that a controlled preoxidation of the silicon nitride powder surface could significantly increase the surface-charging and hence the electrostatic-stabilization behaviour of silicon nitride powder in aqueous solution. Whereas, without surface oxidation, a distinct yield stress of approximately 60 Pa can be observed, this flow stress is drastically decreased with increasing surface-oxide-layer thickness and finally diminished after oxidation for 8 h at 550°C. The decrease in τ_B with decreasing interactive forces (increasing ζ) follows a linear relation between τ_B and ζ^2 as has been reported for other aqueous systems.[16,24] Oxidation for 8 h at 550°C in air was found to result in an oxygen pick-up of 0.9 wt%, which corresponds to a thickness of less than 0.3 nm of a silica-like surface layer.[25] This oxide layer resulted in a significant increase in the zetapotential from $\zeta = -30\,mV$ (as received) to $\zeta = -84\,mV$ (preoxidized) and preferential adsorption of anionogenic polyelectrolytic surfactants at high pH. Figure 2 shows the influence of the surface-oxidation treatment on the rheology of a concentrated slip with $\phi = 0.377$ and $D_{max} = 660\,s^{-1}$ at pH 8. For this reason, the following experiments with highly concentrated slips were carried out only with the preoxidized powder (8 h, 550°C).

Figure 3(a) and (b) shows the flow curves of silicon nitride slips with various solid-volume concentrations, ϕ, ranging from 0.2 to 0.475. The preoxidized silicon nitride was dispersed in water at a pH of 8.5 and a deflocculant concentration of $5 \times 10^{-3}\,ml/g$ (solid). The initial shear rates were $D_{max} = 690\,s^{-1}$ (a) and $D_{max} = 2770\,s^{-1}$ (b), respectively. For $\phi < 0.35$, the flow curves can be ascribed as
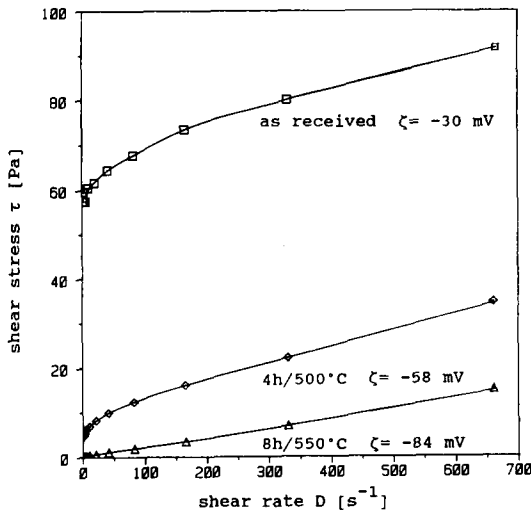
Fig. 2. Shear diagram (shear stress versus shear rate) of the as-received and preoxidized silicon nitride powder in aqueous solution.
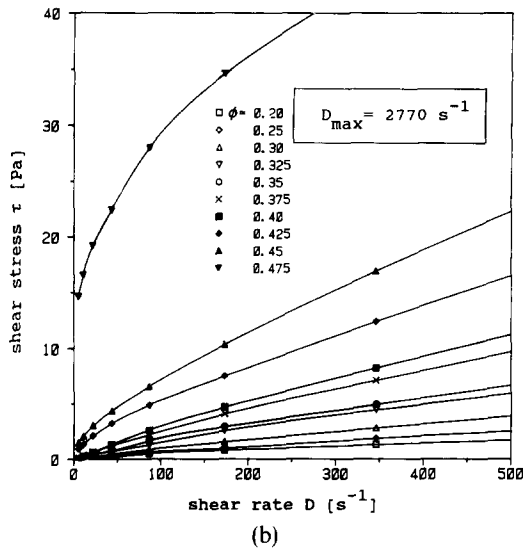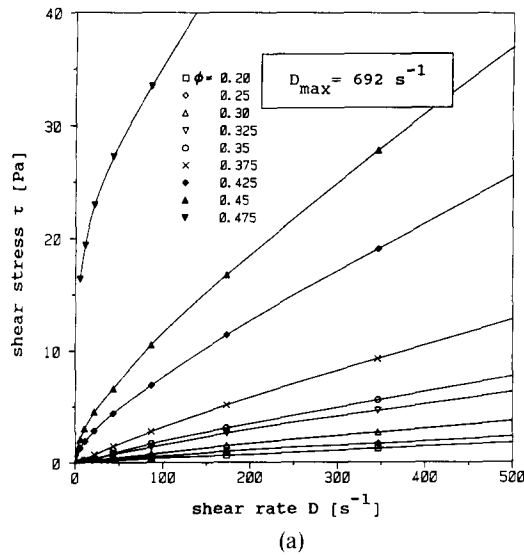

(a)

(b)

Fig. 3. Shear diagram of the aqueous silicon nitride slips with different particle-volume concentrations ϕ from 0·2 to 0·475. The initial shear rates were (a) $D_{max} = 690\,s^{-1}$ and (b) $D_{max} = 2770\,s^{-1}$.

Newtonian with a linear dependence of the shear stress, τ, on the shear rate, D;

$$\tau = \eta_a D \qquad (1)$$

where η_a is the apparent viscosity ($\eta_a = \tau/D = d\tau/dD$ for Newtonian flow). Suspensions with higher particle-volume concentrations, $\phi > 0·35$, exhibit a pseudo-plastic flow behaviour with a Bingham value τ_B:

$$\tau = \tau_B + \eta_{pl} D \qquad (2)$$

where η_{pl} is the plastic viscosity of the system at $D > D_0$. Figure 4 shows the increase in τ_B with ϕ for the two different initial shear rates of $D_{max} = 690$ and $2770\,s^{-1}$. On the basis of the elastic floc model,[17] τ_B may be expressed as a parabolic function of ϕ:

$$\tau_B = K\frac{\eta_s}{r^3}C_{FP}\phi^2 \qquad (3)$$

where η_s is the solvent viscosity, r the particle radius, and K a constant that accounts for the interaction energy between the flow units.[26] The floc-volume ratio, C_{FP}, describes the ratio of solid to trapped liquid and may attain values of $1 < C_{FP} < 7$. Assuming K and C_{FP} to be independent on the particle-volume concentration ϕ, eqn (3) suggests a relationship between τ_B and ϕ^2, which has been confirmed experimentally.[24,27] The data points in Fig. 4, however, could not be reproduced by the calculated curve ($KC_{FP} = 0·1096\,\mu m^3/s$, $\eta_s = 89\,m\,Pa\,s$ at 25°C, $r = 0·14\,\mu m$) at $\phi > 0·35$. The discrepancy between the measured and calculated curves at higher particle-volume concentrations suggests a much stronger dependence of τ_B on ϕ owing to increasing particle–particle interactions, i.e. K and C_{FP} may no longer be assumed to be independent of ϕ. This suggestion is confirmed by the thixotropic behaviour of the silicon nitride slips. No change in τ_B with time could be observed for slips with $\phi < 0·35$,
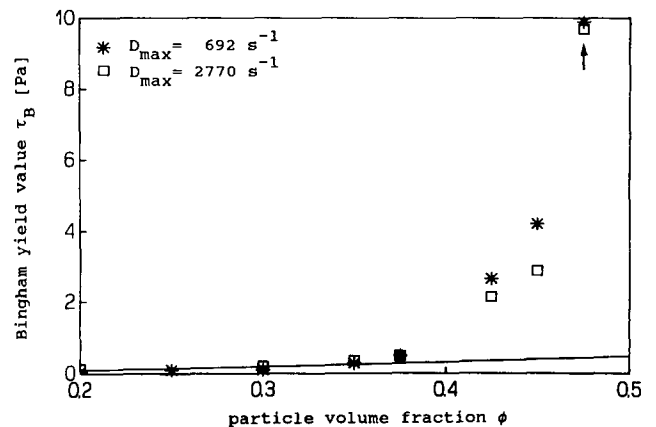

Fig. 4. Extrapolated Bingham-yield values τ_B versus particle-volume concentration of the silicon nitride slips. Calculated curve according to eqn. (3).
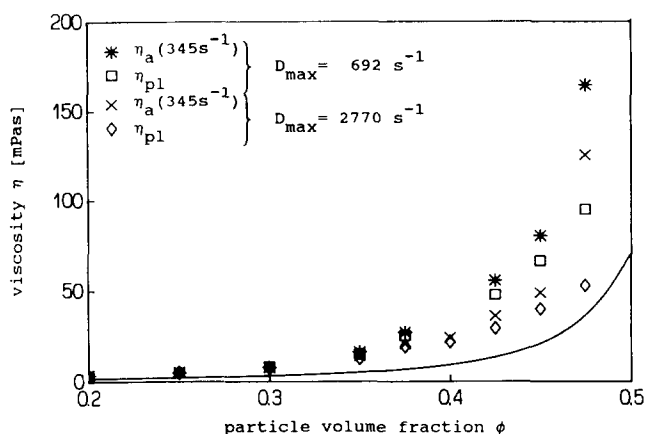
Fig. 5. Apparent, η_a, and plastic viscosity, η_{pl}, versus particle-volume concentration. Calculated curve according to eqn (4).

whereas more highly concentrated slips increased in the value of τ_B. For the slip with $\phi = 0.475$, a Bingham value of τ_B of only 13 Pa was measured after 10 s at $D = 5.4 \text{ s}^{-1}$, which drastically increased to 200 Pa after 30 min.

The results of the viscosity evaluations are summarized in Fig. 5. Both the apparent viscosity η_a at a shear rate of 345 s^{-1} and the plastic viscosity η_{pl}, which is assumed to remain constant with further increase in the shear rate, are given as a function of the particle-volume concentration. The viscosity data were evaluated according to an exponential flow equation derived for higher particle-volume fractions:[20]

$$\eta = \eta_s \exp\left[\frac{2\cdot5\,\phi}{1-\phi/p}\right] \tag{4}$$

which relates the viscosity to the viscosity of the pure solvent, η_s, the particle-volume concentration, ϕ, and a maximum packing density, p, of the flow units. Equation (4) accounts for non-interacting spheres and is often also used to describe the solid-concentration dependence of the viscosity for polydispersed materials [9,17,20,21] with $\phi > 0.1$. The grain-size distribution may be expressed by the powder-packing parameter, p, which reflects the differences in the packing density that are dependent on the grain-size distribution. Theoretical considerations suggested a significant reduction in the viscosity when bi- or multimodal powder mixtures are used instead of monosized powders.[28] With a maximum particle-packing density of $p = 0.7$ taken, the dotted curve in Fig. 5 was calculated. The values of the viscosity fall well above the curve for non-interacting spherical particles, as it is to be expected for strongly interacting systems.[29] Even for smaller values of p, which, however, will no longer be realistic as maximum packing densities, the measured viscosity behaviour could not be reproduced at

intermediate and high particle-volume concentrations ($\phi > 0.35$).

4 Discussion

While the experimental data for τ_B and η of aqueous silicon nitride suspensions of low concentrations ($\phi < 0.35$) may well be described by eqn (4), more highly concentrated suspensions increasingly deviate from the calculated curves. To describe the flow behaviour of concentrated silicon nitride suspensions with increasing particle–particle interactions, a model consisting of flocced aggregates is considered, where the floc structure is dependent on the particle-volume concentration. By analogy with the model of regular solutions in thermodynamics, the rheological interactions in a higher concentrated suspension may be separated into two energy dissipating processes: (i) the colloidal interactions between particles and (ii) the molecular interactions between the liquid molecules as for A and B atoms in the thermodynamics of solutions. The ideal solution then corresponds to a suspension in which the colloidal particle–particle interactions are only of a repulsive or neutral nature. For this limiting case, only the purely hydrodynamic forces in the suspension may be determining the viscosity, and hence eqn (4) may successfully be applied. The tendency for phase separation in thermodynamics, when the A–A and B–B interactions are considerably stronger than two A–B interactions, then corresponds to the flocculation of the suspension, which may be regarded as a phase separation. In this case, the attractive forces between two colloidal-powder particles are stronger than those between the liquid molecules and the powder particles. Colloidal-consolidation processes may therefore be described as phase transformations in one-component colloidal systems, for which phase diagrams have been proposed.[30]

For colloidal suspensions, the effective floc-volume concentration, ϕ_F, corresponds to the activity a_i, which is related to the particle-volume concentration ϕ by the specific floc-volume factor C_{FP} so that it may be written:

$$\phi_F = C_{FP}\phi \tag{5}$$

In the elastic-floc model, C_{FP} accounts for spherical flocs having an essentially constant ratio of solid-to-trapped liquid.[17] For ϕ approaching the geometrical packing density p, the viscosity must approach infinity, and even slow shear rates will result in high shear stresses owing to the predominance of the

hydrodynamic forces. No flocs exist, and the first boundary condition is:

$$\lim_{\phi \to p} C_{FP}(\phi) = 1 \tag{6}$$

which is satisfied by an expression equivalent to the activity variation with concentration in regular-solution thermodynamics:

$$C_{FP} = \exp\left\{M\left(1 - \frac{\phi}{p}\right)^2\right\} \tag{7}$$

For very dilute suspensions, $\phi \to 0$, however, the boundary condition is given by:

$$\lim_{\phi \to 0} C_{FP} = C_{FP}^0 \tag{8}$$

where C_{FP}^0 is an initial floc-volume ratio independent of ϕ and corresponds to C_{FP} in the elastic-floc model.[17] The parameter C_{FP}^0 may attain values between 1 (fully isolated particles) and $e^2 = 7\cdot4$. The constant M in eqn (7) accounts for the colloidal-interaction energies between the particles, which for $\phi \to 0$ may be expressed as $M = \ln C_{FP}^0$. Substituting M into eqn (7) results in:

$$C_{FP} = C_{FP}^0\left(1 - \frac{\phi}{p}\right)^2 \tag{9}$$

Combining eqn (9) with eqn (5) finally provides an expression for the floc-volume concentration ϕ_F as a function of the particle-volume concentration, ϕ:

$$\phi_F = \phi C_{FP}^0\left(1 - \frac{\phi}{p}\right)^2 \tag{10}$$

Figure 6 shows the effective floc-volume concentration, ϕ^F, plotted against the particle-volume concentration, ϕ, for different values of C_{FP}^0 in the
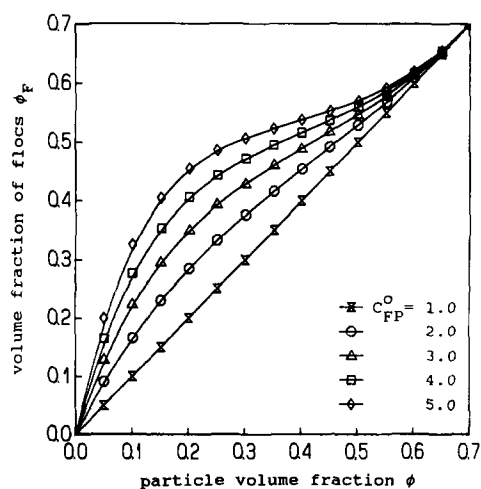
range 1–5 at a constant geometrical-packing density of $p = 0\cdot7$. This graph is analogous to the activity isotherms of a regular solution in thermodynamics. For low solid-volume concentrations, ϕ, the specific floc-volume factor $C_{FP} = \phi_F/\phi$ is almost constant and fits well with the low-concentration region, $\phi < 0\cdot1$, where the elastic-floc model sufficiently describes the influence of the particle-volume concentration. As concluded earlier from experimental-rheology measurements, the assumption $C_{FP} \approx$ constant is restricted to low solid concentrations.[15,16] This may be immediately seen from Fig. 6. For solid concentrations as high as the geometrical-packing density p, the colloidal-interaction forces at a constant shear rate may be regarded as negligible compared with the shear forces that arise from friction and plastic deformation among the particles. The flocs will be destroyed by the shear motion, resulting in an approach of the curves for different values of C_{FP}^0 for $\phi \to p$ in Fig. 6.

The concentration-dependent effective floc-volume concentrations, ϕ_F, as expressed by eqn (10) may directly be used in eqn (4) instead of the particle-volume concentration ϕ, so that eqn (4) may be rewritten for the relative viscosity η_r as:

$$\eta_r = \frac{\eta}{\eta_s} = \exp\left[2\cdot5\left\{\phi^{-1}C_{FP}^0 - \left(1 - \frac{\phi}{p}\right)^2 - p^{-1}\right\}^{-1}\right] \tag{11}$$

Figure 7 shows a plot of η_r plotted against ϕ for various values of C_{FP}^0 from 1 to 5 and $p = 0\cdot7$. It can be seen that the relative viscosity strongly increases with the degree of flocculation C_{FP}^0 at low and intermediate particle-volume concentrations, ϕ. Changing the packing density, p, of the flocs (Fig. 8) reveals a significant influence on η_r only above

Fig. 6. Volume fraction of flocs, ϕ_F, versus particle-volume concentration for different initial floc-volume ratios, $C_{FP}^0 = 1$–5. The curves were calculated according to eqn (10) with a constant packing density of $p = 0\cdot7$.
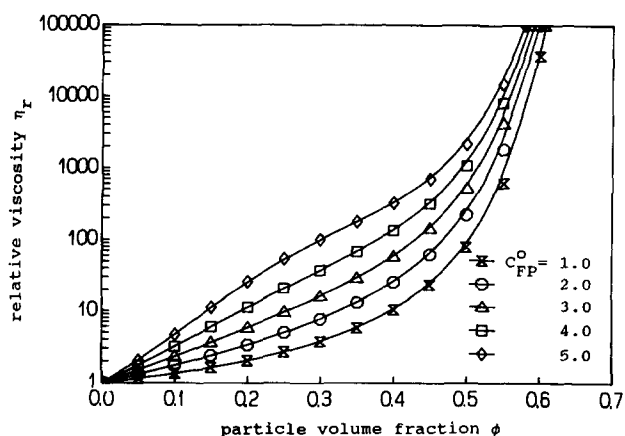

Fig. 7. Relative viscosity versus particle-volume concentration for different initial floc-volume ratios $C_{FP}^0 = 1$–5, but a constant packing density $p = 0\cdot7$, calculated according to eqn (11).
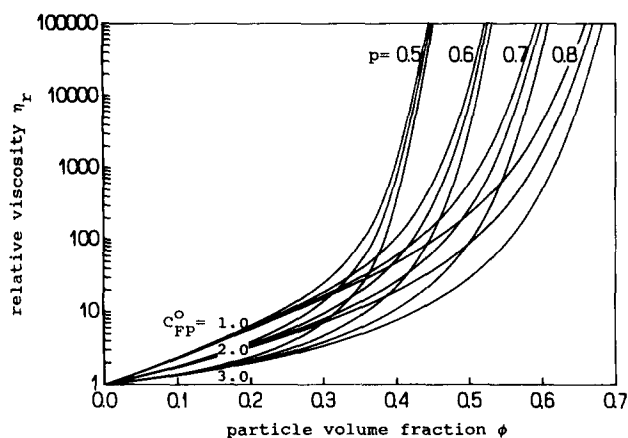
Fig. 8. Relative viscosity, η_r, versus particle-volume concentration for different particle-packing densities $p = 0.5$–0.8, calculated according to eqn (11).

$\phi > 0.3$, whereas, at lower particle-volume concentrations, η_r remains almost unaffected by p. At low particle-volume concentrations, C_{FP}^0 exerts the major influence on η_r, whereas at high concentrations p dominates. The critical particle-volume concentration coincides roughly with the experimentally observed behavioral transition from linear to pseudo-plastic flow behaviour of the silicon nitride slips at $\phi = 0.35$. As can be seen from Fig. 9, the calculated curve with $p = 0.7$ and $C_{FP}^0 = 2$ reproduces the experimental values in the whole particle-volume concentration range, ϕ, from 0.2 to 0.475. A C_{FP}^0 value of 2 represents a high-density floc structure,[15,16] with a solid fraction in floc of approximately 0.55. For $C_{FP}^0 = 1$, eqn (4) provides results for isolated particles, which, however, could not satisfactorily describe the concentration-dependence of the experimentally measured slip viscosities.

The resulting flow equation of the aqueous silicon nitride slips, eqn (11), is determined by only two structural parameters: the initial floc-volume coefficient, C_{FP}^0, and the packing density, p. The former
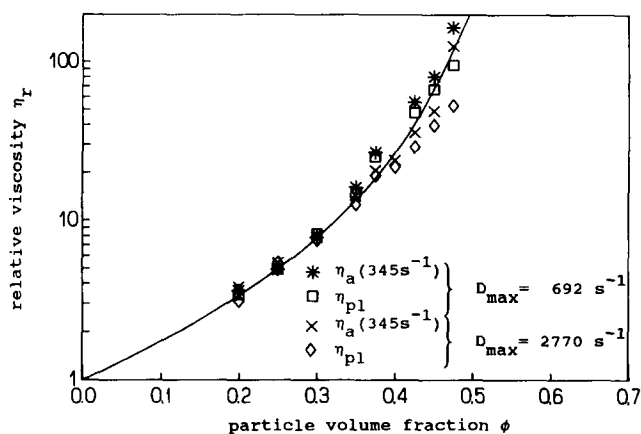

Fig. 9. Experimental and calculated (eqn (11)) values of relative viscosity versus particle-volume concentration.

quantity is related to the electrochemical interparticle bonding forces, and the packing density refers to the particle–particle hydrodynamic interactions. The shear-dependent floc-structure dynamics at low particle-volume concentrations seems to be primarily influenced by the electrochemical interaction, whereas in highly concentrated slips the hydrodynamic interactions seem to gain in significance in their effect on the rheological behaviour. The electrochemical interparticle forces of silicon nitride in aqueous solution are dominated by electrostatic repulsion (ζ^2),[27] which may be controlled by pH and surface adsorption of ionogenic polyelectrolytes.[23] The hydrodynamic inter-particle forces, however, depend on the solvent viscosity and the hydrodynamic particle radius (r^2),[31] so that the effects of particle-size distributions, surface coatings, and the solvent properties have to be considered in more detail in order to develop highly concentrated silicon nitride slips with improved rheological properties.

5 Conclusions

The rheological behaviour of aqueous silicon nitride slips stabilized by an anionic polyelectrolyte at pH > 8 may be characterized by two distinct regions: at low particle-volume concentrations, $\phi < 0.35$, the flow curves are linear, and the slips are characterized as Newtonian, whereas at higher particle-volume concentrations a pseudo-plastic behaviour occurs. Neither the Bingham-yield value nor the plastic viscosity could be explained by the flow equations of the elastic-floc model, where a linear dependence of the floc volume on the particle-volume concentration is assumed. By introducing an effective specific floc volume, which depends only on the particle-volume concentration and the packing density, an expression for the relative viscosity was derived, which fits very well with the experimental values from low to high particle-volume concentrations.

In contrast to the elastic-floc model, where the floc size is assumed to be constant and essentially unaffected by the modest shear rates $(100–2000\,\mathrm{s}^{-1})$, in the silicon nitride slips aggregates of flocs will be formed at these shear rates. This may indicate much stronger colloidal interactions at higher particle-volume concentrations than are expected from the electrokinetic measurements in diluted systems. In addition to the hydrodynamic interactions, chemical interactions, such as the dissolution of impurities in the powder, may increasingly influence the

particle–particle interactions with the solids concentration.

References

1. Aksay, I. A. & Schilling, C. H., Mechanics of colloidal filtration. In *Advances in Ceramics*, ed. J. A. Mangels. American Ceramic Society, Columbus, Ohio, USA, 1984, pp. 85.

2. Aksay, I. A., Microstructure control through colloidal filtration. In *Advances in Ceramics*, ed. J. A. Mangels. American Ceramic Society, Columbus, Ohio, USA, 1984, pp. 94.

3. Rubin, A. J., Formation and stability of colloidal dispersions of fine particles in water. In *Emergent Process Methods for High Technology Ceramics*, ed. R. F. Davis, H. Palmour III & R. L. Porter, Plenum Press, New York, 1984; p. 45.

4. Vincent, B., The effect of adsorbed polymers on dispersion stability, *Adv. Coll. Interf. Sci.*, **4** (1974) 193.

5. Sato, T. & Ruch, R., *Stabilization of Colloid Dispersions by Polymer Adsorption.* Marcel Dekker, New York, 1980.

6. Bleier, A., Fundamentals of preparing suspensions of silicon and related ceramic powders. *Comm. Am. Ceram. Soc.*, **66** (1983) C-79.

7. Nagel. A., Schlickergießen von sinterfähigen Siliciumnitrid-Keramiken. PhD thesis, University of Stuttgart, 1988.

8. Adcock, D. S. & McDowall, I. C., The mechanism of filter pressing and slip casting, *J. Am. Ceram. Soc.*, **40** (1957) 355.

9. Goodwin, J. W., The rheology of dispersions. *Colloid Sci.*, **2** (1975) 246.

10. Hiemenz, P. C., *Principles of Colloid and Surface Chemistry.* Marcel Dekker, New York 1981.

11. Parfitt, G. D., *Dispersion of Powders in Liquids.* Applied Science Publishers, New York, 1981.

12. Bleier, A., The science and interactions of colloidal particles and ceramic processing. In *Emergent Process Methods for High Technology Ceramics*, ed. R. F. Davis, H. Palmour III & R. L. Porter. Plenum Press, New York, 1984, p. 71.

13. Overbeck, J. T. G., How colloid stability affects the behavior of suspensions. In *Emergent Process Methods for High Technology Ceramics*, ed. R. F. Davis, H. Palmour III & R. L. Porter. Plenum Press, New York, 1984, p. 25.

14. Rabinovich, E. M., Leitner, S. & Goldenberg, A., Slip casting of silicon nitride for pressureless sintering. *J. Mater. Sci.*, **17** (1982) 323.

15. Firth, B. A., Flow properties of coagulated suspensions. II: Experimental properties of the flow curve parameters. *J. Colloid Interf. Sci.*, **57** (1976) 257.

16. Firth, B. A. Hunter, R. J., Flow properties of coagulated colloidal suspensions. I: Energy dissipation in the flow units; III: The elastic floc model. *J. Colloid Interf. Sci.*, **57** (1976) 248, 266.

17. Hunter, R. J., The flow behavior of coagulated colloidal dispersions. *Adv. Colloid Interf. Sci.*, **17** (1982) 197.

18. Michaels, A. S. Bolger, J. C., The plastic flow behavior of flocculated suspensions. *Ind. Engng Chem. Fund.*, **1** (1962) 197.

19. Chou, C. C. & Senna, M., Correlation between rheological behavior of aqueous suspensions of Al_2O_3 and properties of cast bodies: effect of dispersant and ultrafine powders. *Am. Ceram. Soc. Bull.*, **66** (1987) 1129.

20. Mooney, M., The viscosity of concentrated suspension of spherical particles. *J. Colloid Sci.*, **6** (1951) 162.

21. Rutgers, J. R., Relative viscosity and concentration. *Rheol. Acta*, **2** (1962) 305.

22. Papenkuizen, J., van der Schee, H. A. & Fleer, G. J., Polyelectrolyte adsorption. I: A new lattice theory. *J. Colloid Interf. Sci.*, **104** (1985) 540.

23. Hunter, R. J., *Zeta Potential in Colloid Science.* Academic Press, London, 1981.

24. Hunter, R. J. & Nicol, S. K., Dependence of plastic flow behavior of clay suspensions on the phase properties. *J. Colloid Interf. Sci.*, **28** (1968) 250.

25. Greil, P., Processing of silicon nitride ceramics. *Mater. Sci. Engng*, **A109** (1989) 27.

26. Gillespie, T., An extension of Goodeve's impulse theory of viscosity to pseudoplastic systems. *J. Colloid Sci.*, **15** (1960) 219.

27. Friend, J. P. & Hunter, R. J., Plastic flow behavior of coagulated suspensions treated as a preptization phenomenon. *J. Colloid Interf. Sci.*, **37** (1971) 548.

28. Farris, R. J., Prediction of the viscosity of multimodal suspensions from unimodal viscosity data. *Trans. Soc. Rheol.*, **12** (1968) 281.

29. Krieger, I. M., Rheology of monodisperse lattices. *Adv. Colloid Interf. Sci.*, **33** (1972) 111.

30. Aksay, I. A. & Schilling, C. M., Colloidal filtration route to uniform microstructures. In *Ultrastructure Processing of Ceramics, Glasses, and Composites*, ed. L. L. Hench & D. R. Ulrich. John Wiley, New York, 1984, p. 439.

31. Goren, S. L., Hydrodynamic forces on touching spheres along line of centers exerted by a shear field. *J. Colloid Interf. Sci.*, **36** (1971) 94.